



## INFLUENCE OF THE INLET TEMPERATURE ON THE EFFICIENCY OF A FLAT-PLATE SOLAR COLLECTOR DURING ONE YEAR IN BRAZIL

**Bárbara Vilhena Costa Neves**

**Hairton Júnior José da Silveira**

**Cristiana Brasil Maia**

Pontifícia Universidade Católica de Minas Gerais - PUC, Belo Horizonte, Minas Gerais, Brasil

barbaravilhena.neves@gmail.com

hairtonjjsilveira@gmail.com

cristiana@pucminas.br

**Abstract.** *The increase of the energy demand, along with the depletion of conventional energy sources, has led to a search for renewable energy sources. Among the renewable energy resources, solar energy arises as a potential source, due to its inexhaustibility and green property. One of the most important domestic applications of the solar energy is the solar water heating system. Flat plate solar collectors are devices that convert solar radiation into heat for a wide range of applications specifically in domestic and industrial usages, such as bathing, washing and heating. They are simple in design, use both beam and diffuse components of solar radiation, do not require tracking of the sun, and require little maintenance. In this paper, a mathematical model is developed regarding the efficiency and the outlet water temperature of a flat-plate solar collector, over a year in Brazil. The dimensions of the device were defined as those of a typical collector. The software EES (Equation Engineering Solver) was used to simulate the hourly and average daily and monthly efficiencies for the city of Belo Horizonte (latitude 19°55'S and longitude 43°56'W), during the daylight hours of 365 days. The hourly incident solar radiation was predicted using the daily clearness index (Kt) based on the typical meteorological year obtained from the literature. The ambient temperature was assumed constant, and equal to the average annual value described in the literature. This paper also seeks to analyze the effects of the inlet water temperature of the system (25, 30, 35 and 40 °C) on the efficiency and outlet water temperature. It is expected that a decrease in the inlet water temperature will lead to an increase in the collector's efficiency and to a decrease in the exit water temperature. Also, it is expected that the monthly efficiency increases with the incident solar radiation.*

**Keywords:** *efficiency, solar collector, useful gain, inlet temperature, clearness index.*

### 1. INTRODUCTION

The increase of the use of renewable energy sources has been due to growth of the population, as well as the present limitation on conventional sources to provide the energy needed in the global system. Fossil energies bring negative effects to the environment, such as: air pollution, global warming, degradation of the ozone layer, and the greenhouse effect (Sözen *et al*, 2008). Therefore, solar energy, coming from the sun in the form of solar radiation, can be an interesting alternative to replace fossil energies, without aggression to the environment.

A solar collector is a device used to convert the radiation of the sun into heat through an absorber plate and a working fluid. The heat generated by the collector can be used to heat water, and this heated water can be used for baths, environment heat, and industrial processes. Particularly, the flat plate solar collector for water heating is the most used collector in the world (Tong *et al*, 2020), but in some cases it can have limitations due to little space available. This problem can be solved by increasing the efficiency of the collector to reach the needs of the situation.

In technical literature, it is possible to find several research studies about how to increase the efficiency on a flat plate solar collector. Maia *et al* (2014) studied how to increase efficiency by maximizing the absorbed solar energy by modifying the position of the solar collector using a tracking system. It was observed that the tracking system with rotation about two axes showed higher absorbed energy and efficiency. The solar collector in a fixed tilt angle, facing north, presented the lower values of efficiency.

Diego-Ayala *et al* (2016) explored experimentally how the mass flow on a solar collector can influence the efficiency. Two methods were used in the comparison: observing the water under thermosyphon conditions and by a submersible pump (forced flow). The results showed that the greater values on efficiency were found when the water heater was working under forced flow. The authors suggest that a miniature submersible pump to force the flow would improve significantly the efficiency on a flat plate solar collector as also would reduce the temperature differential.

The use of nanofluids has been a good alternative to implement on solar collectors as working fluid. Nanofluids are obtained when nano-sized particles (mostly metallic) are added to a base fluid. This nanoparticle increases the heat transfer of the fluid, bringing higher values of absorption of incident radiation on solar collectors (Tyagi *et al* 2009). He

*et al* (2015) researched the influence of the size of these nanoparticles on the efficiency of solar collectors. It was observed in the tests performed, a decrease on the efficiency with the increase on the size of the particle.

Müller *et al* (2019) presented a numerical study of the comparison of the efficiency of a flat plate solar collector using several commercially available absorber coatings. These coatings were categorized as: based on black chrome, highly selective coatings, solar paints and thermochromic coatings. The coatings were compared in application for a domestic system using a tapping volume of 100 L. The results indicated an increase in the auxiliary energy demand: 6% for black chrome, 7% for thermochromic and 21% for solar paint coatings. This study also showed that the spectral selectivity of solar absorbers has an influence on the efficiency.

Bhowmik *et al* (2017) present a study using a new technology to increase the performance of a flat plate solar collector. The use of reflector can improve the reflectivity of the collector due to its capacity of concentrating both direct and diffuse radiation. Seeking to upgrade the intensity of incident radiation it was used a reflector able to move in an hourly basis along the day, tracking the sun. It was constructed a prototype with and without the reflector and the use of the reflector demonstrated an increase of 10% on the efficiency of the collector, proving that this can be applied as one method to improve the performance of a flat plate solar collector.

Garcia *et al* (2019) observed the influence of convective barriers on the efficiency of flat plate solar collectors. The introduction of these convective barriers was made putting them between the absorber plate and the glass cover, limiting the space between them. This use of convective barriers seeks to reduce the heat losses to the environment and the study showed that with a satisfactory number of barriers these can improve the efficiency for some situations.

Sözen *et al* (2008) proposed an analyze using neural network approach to determine the efficiency of a flat plate solar collector. Artificial neural network are computational models that are normally used to develop and solve complex functions, due to this method have the characteristic to learn from examples, be more speed and simpler. The paper demonstrated an estimation of a new formula for calculate the efficiency which is also depended on working parameters.

In this study, the software EES (Equation Engineering Solver) was used to develop a mathematical model to increase the efficiency of a flat plate solar collector based on the model described by Duffie and Beckman (2013), in which the mean absorber plate temperature is solved in an iterative procedure involving the collector overall loss coefficient. By using this iterative procedure, it was possible to analyze the influence of different inlets water temperature of the system (25, 30, 35 and 40°C) on the efficiency and outlet water temperature. The ambient temperature was assumed constant, and equal to the average annual value described in the literature by the location of Belo Horizonte.

This mathematical model was also developed simulating the hourly and average daily and monthly for the city of Belo Horizonte, during the daylight hours of 365 days, observing the influence of these factors on the efficiency and the outlet water temperature of the collector.

## 2. MATHEMATICAL MODEL

In this paper, a mathematical model was developed to study the efficiency, in state conditions, of a solar flat plat collector based on Duffie and Beckman (2013). The efficiency ( $\eta$ ) can be defined as the relation between the useful gain ( $Q_u$ ), the area of the collector ( $A_c$ ) and the incident radiation ( $G_T$ ), Eq. (1).

$$\eta = \frac{\int Q_u dt}{A_c \int G_T dt} \quad (1)$$

### 2.1 Calculation of useful heat using the removal factor

The instant useful gain ( $Q_u$ ) was calculated by using the collector area ( $A_c$ ), the absorbed radiation ( $S$ ), the overall loss coefficient ( $U_L$ ), the mean absorber plate temperature ( $T_{pm}$ ) and the ambient temperature ( $T_a$ ), in Eq. (2).

$$Q_u = A_c [S - U_L(T_{pm} - T_a)] \quad (2)$$

It was used as the ambient temperature ( $T_a$ ) the maximum average for the city Belo Horizonte equal to 22.9°C Meteornorm (2012).

The overall loss coefficient ( $U_L$ ), in Eq. (3) was calculated regarding the top loss coefficient ( $U_t$ ) which includes the losses by convective and radiative losses to the environment by the top of the collector, the bottom loss coefficient ( $U_b$ ) which includes the losses by convective and radioactive to the environment by back of the collector and the heat transfer coefficient on the edge ( $U_e$ ).

$$U_L = U_t + U_b + U_e \quad (3)$$

$$U_t = \left[ \frac{N}{\frac{C}{T_{pm}} \left( \frac{T_{pm} - T_a}{N + f} \right)^e + \frac{1}{h_w}} \right]^{-1} + \frac{\sigma(T_{pm} + T_a)(T_{pm}^2 + T_a^2)}{\epsilon_p + 0,00591N h_w + \frac{2N + f - 1 + 0,133\epsilon_p}{\epsilon_c}} \quad (4)$$

$$f = (1 + 0,089h_w - 0,1166h_w\epsilon_p)(1 + 0,07866N) \quad (5)$$

$$C = 520(1 - 0,000051\beta^2) \quad (6)$$

$$e = 0,430 \left(1 - \frac{100}{T_{pm}}\right) \quad (7)$$

$$U_b = \frac{K}{L} \quad (8)$$

$$U_e = \frac{\frac{k_{iso}As}{e_{iso}}}{A_c} = \frac{\frac{k_{iso}Pe_{col}}{e_{iso}}}{wL} \quad (9)$$

Some of the variables evolved are: the tilt angle of the collector ( $\beta$ ) equals  $20^\circ$ , the number of covers (N) equals 1, the emittance of the glass ( $\epsilon_c$ ) equals 0.80, the emittance of the plate ( $\epsilon_p$ ) equals 0.90, the insulation conductivity ( $k_{iso}$ ) equals 0.050 W/mK, the edge insulation thickness ( $e_{iso}$ ) equals 25 mm, the collector thickness ( $e_{col}$ ) equals 75 mm, the collector bank length (L) equals 2 m, the collector bank width (w) equals 1 m, the perimeter of the collector (P) equals 6 m and the wind heat transfer convective ( $h_w$ ) equals 10 W/m<sup>2</sup>K. These values were selected based on typical commercial solar collectors, as defined by Maia et al. (2014).

## 2.2 Calculation of absorbed radiation using transmittance-absorptance product

The absorbed radiation (S) was calculated in Eq. (10), by the sum of the transmittance-absorptance product times the incident radiation for beam, diffuse and ground reflected components. The incident solar radiation is represent by:  $I_b$  for the beam component and  $I_d$  for the diffuse one. The slope angle of the collector is the  $\beta$ , the ground for reflectance is the  $\rho_g$ , the geometric factor is  $R_b$  and  $(\tau\alpha)_b$ ,  $(\tau\alpha)_d$  and  $(\tau\alpha)_g$  are the transmittance-absorptance products for the beam, diffuse and ground-reflected radiation, respectively.

$$S = I_b R_b (\tau\alpha)_b + I_d (\tau\alpha)_d \left(\frac{1+\cos\beta}{2}\right) + \rho_g (I_b + I_d) (\tau\alpha)_g \left(\frac{1-\cos\beta}{2}\right) \quad (10)$$

The transmittance-absorptance product ( $\tau\alpha$ ) is given by Eq. (11). It is important to describe that  $\rho$  is the reflectance and the value is always from ground reflected component.

$$(\tau\alpha) = \frac{\tau\alpha}{1-(1-\alpha)\rho} \quad (11)$$

The absorptance ( $\alpha$ ) was calculated using Eq. (12) as describe in Beckman *et al* (1977) and  $\alpha_n$  was assumed 0.95.

$$\frac{\alpha}{\alpha_n} = 1 - 1,5879x10^{-3}\theta_1 + 2,7314x10^{-4}\theta_1^2 - 2,3026x10^{-5}\theta_1^3 + 9,0244x10^{-7}\theta_1^4 - 1,8x10^{-8}\theta_1^5 + 1,7734x10^{-10}\theta_1^6 - 6,9937x10^{-13}\theta_1^7 \quad (12)$$

The overall transmittance of the cover ( $\tau$ ) depends of the beam, diffuse or ground reflected component of the incident radiation and its value is given by the absorption ( $\tau\alpha$ ) times the transmittance ( $\tau_r$ ) of the glass. It was used Bouguer's law for calculate the absorption of the glass, this was resulted on Eq. (13).

$$\tau_a = \exp\left(-\frac{KL}{\cos\theta_2}N\right) \quad (13)$$

The transmittance of the glass is calculated by Eq. (14) and it is function of parallel reflectance ( $r_{II}$ ) and perpendicular reflectance ( $r_I$ ), calculated respectively by Eqs. (15) and (16).

$$\tau_r = \frac{1}{2} \left[ \frac{1-r_{II}}{1+(2N-1)r_{II}} + \frac{1-r_I}{1+(2N-1)r_I} \right] \quad (14)$$

$$r_{II} = \frac{\tan^2(\theta_2-\theta_1)}{\tan^2(\theta_2+\theta_1)} \quad (15)$$

$$r_I = \frac{\sin^2(\theta_2-\theta_1)}{\sin^2(\theta_2+\theta_1)} \quad (16)$$

These equations used: the number of covers (N), the glass thickness (L) and K that is proportionality constant called extinction coefficient, which depends on the glass type, it was assumed  $20 \text{ m}^{-1}$ . Besides that, it was used the angle of incident ( $\theta_1$ ) and the angle of the glass refraction ( $\theta_2$ ) and they are related by Snell's law in Eq. (17) that also used the refractive index of air ( $n_1$ ) and the refractive index of glass ( $n_2$ ).

$$n_1 \sin \theta_1 = n_2 \sin \theta_2 \quad (17)$$

The incident angle for diffuse component ( $\theta_d$ ) is calculated using Eq. (18) and for the incident angle for ground component it was used Eq. (19). These equations used the local latitude ( $\phi$ ) as  $-20^\circ\text{S}$  and the angle indicative of the day of the year called declination ( $\delta$ ) was calculated by equation of Copper (1969).

$$\theta_d = 59,7 - 0,1388\beta + 0,001497\beta^2 \quad (18)$$

$$\theta_g = 90 - 0,5788\beta + 0,002693\beta^2 \quad (19)$$

$$\cos \theta = \cos(\phi + \beta) \cos \delta \cos \omega + \sin(\phi + \beta) \sin \delta \quad (20)$$

$$\delta = 23,45 \sin \left[ \frac{360}{365} (n + 284) \right] \quad (21)$$

### 2.3 Calculation of the total incident radiation using the clearness index and applying the isotropic sky model

The total hourly radiation ( $I_T$ ) is described as the radiation incident on the sloped surface of the collector during daylight hours and was calculated using the reflectance from the ground ( $\rho_g$ ) by the Eq. (22).

$$I_T = I_b R_b + I_d \left( \frac{1 + \cos \beta}{2} \right) + I \rho_g \left( \frac{1 + \cos \beta}{2} \right) \quad (22)$$

The geometric factor ( $R_b$ ) can be describe as a correlation between the ratio of beam radiation on a tilted surface and the beam radiation on the horizontal surface, it was calculated using Eq. (23).

$$R_b = \frac{\cos \theta}{\cos \theta_z} \quad (23)$$

$$\cos \theta_z = \cos \phi \cos \delta \cos \omega + \sin \phi \sin \delta \quad (24)$$

$$\cos \theta = \cos(\phi + \beta) \cos \delta \cos \omega + \sin(\phi + \beta) \sin \delta \quad (25)$$

The hourly radiation (I) was estimated from daily radiation (H) in Eq. (26). The sunset hour angle ( $\omega_s$ ) was used for calculation of the hourly radiation (I) and the diffuse component of the hourly radiation (Id).

$$r_t = \frac{I}{H} \quad (26)$$

$$r_t = \frac{\pi}{24} (a + b \cos \omega) \frac{\cos \omega - \cos \omega_s}{\sin \omega_s - \frac{\pi \omega_s}{180} \cos \omega_s} \quad (27)$$

$$a = 0,409 + 0,5016 \sin(\omega_s - 60) \quad (28)$$

$$b = 0,6609 - 0,4767 \sin(\omega_s - 60) \quad (29)$$

The diffuse component of the hourly radiation (Id) was calculated from the diffuse component of the daily radiation (Hd) in Eq. (30).

$$r_d = \frac{I_d}{H_d} \quad (30)$$

$$r_d = \frac{\pi}{24} \frac{\cos \omega - \cos \omega_s}{\sin \omega_s - \frac{\pi \omega_s}{180} \cos \omega_s} \quad (31)$$

The daily radiation (H) was calculated using Eq. (32). The diffuse component of daily radiation (Hd) was calculated based on Erbs *et al* (1982) which can be applied for  $\omega_s \leq 81.4^\circ$  Eq. (33) and for  $\omega_s > 81.4^\circ$  Eq. (34).

In this study the hourly incident solar radiation was predicted using the daily clearness index (Kt). The clearness index (Kt) is the ratio between the radiation at the site and the extraterrestrial radiation, this value is an indirect measure of the cloudiness of the local and it can be estimated using a historical series of radiation data. In this paper was adopted daily values on the year, based on the radiation data from the Typical Meteorological Year (TMY) for the city of Belo Horizonte. The TMY adopted is based in data from a 30 years series of 1973 to 2002, made available by U.S. Department of Energy.

$$Kt = \frac{H}{H_o} \quad (32)$$

$$\frac{H_d}{H} = \begin{cases} 1,0 - 0,2727Kt + 2,4495Kt^2 - 11,9514Kt^3 + 9,3879Kt^4 & \text{para } Kt < 0.715 \\ 0,143 & \text{para } Kt \geq 0.715 \end{cases} \quad (33)$$

$$\frac{H_d}{H} = \begin{cases} 1,0 + 0,2832Kt - 2,5557Kt^2 + 0,8448Kt^3 & \text{para } Kt < 0.722 \\ 0,175 & \text{para } Kt \geq 0.722 \end{cases} \quad (34)$$

The daily extraterrestrial radiation ( $H_o$ ) can be calculated by integrating the normal incident solar radiation over the period from sunrise to sunset, this integration result in Eq. (35).

$$H_o = \frac{24 \cdot 3600 \cdot G_{sc}}{\pi} \left[ 1 + 0,033 \cos \left( \frac{360}{365} n_{day} \right) \right] \left( \cos \phi \cos \delta \sin \omega_s + \frac{\pi \omega_s}{180} \sin \phi \sin \delta \right) \quad (35)$$

The normal incident solar radiation ( $G_o$ ) was calculated using Eq. (36).

$$G_o = G \cos w_z = G(\cos \phi \cos \delta \cos \omega + \sin \phi \sin \delta) \quad (36)$$

The extraterrestrial radiation (G) describe the total amount of radiation that arrive in the outer surface of the atmosphere. It was calculated using Eq. (37) which depends on the time of the year due the variation on earth-sun distance. This paper will assume a fixed solar constant of 1367 W/m<sup>2</sup>, as adopted by the World Radiation Center.

$$G = G_{sc} \left[ 1 + 0,33 \cos \left( \frac{360}{365} n_{day} \right) \right] \quad (37)$$

## 2.4 Mean absorber temperature

It is important to describe that the mean absorber temperature  $T_{pm}$ , was solved in an interative manner between the Eq. (38) and the Eq. (2). Equation 41 describe how to calculate the mean absorber plate by using the removal factor ( $F_R$ ), the overall loss coefficient ( $U_L$ ), the useful gain ( $Q_u$ ), the fluid inlet temperature ( $T_{fi}$ ) and the collector area ( $A_c$ ).

$$T_{pm} = T_{fi} + \frac{Q_u/A_c}{F_R U_L} (1 - F_R) \quad (38)$$

In this paper it was observed how the inlet temperature ( $T_{fi}$ ) influenced on the behavior of the efficiency and on the mean absorber temperature ( $T_{pm}$ ). It was used 25, 30, 35 and 40°C as the values of the inlet temperature.

The removal factor ( $F_R$ ), in Eq. (39), considers the actual useful energy gain to the energy gain if the whole collector surface were at the fluid inlet temperature. The  $\dot{m}$  is the mass flow rate,  $C_p$  is the specific heat of water and  $F'$  is the collector efficiency factor.

$$F_R = \frac{\dot{m} C_p}{A_c U_L} \left[ 1 - \exp \left( - \frac{A_c U_L F'}{\dot{m} C_p} \right) \right] \quad (39)$$

$$F' = \frac{1/U_L}{W \left( \frac{1}{U_L |D_o + (W - D_o) F'} + \frac{1}{\pi D_i h_{fi}} \right)} \quad (40)$$

$$F = \frac{\tanh[m(W - D_o)/2]}{m(W - D_o)/2} \quad \text{and} \quad m = \sqrt{\frac{U_L}{K_p d}} \quad (41)$$

### 3. RESULTS

In order to observe the influence of the inlet temperature on the efficiency of a flat plate solar collector, it was developed a routine on EES (Engineering Equation Solver). The simulation was run in an hourly basis, for the 365 days of the year. The slope of the solar collector was fixed in 20°, equal to the latitude of the location (Belo Horizonte, Brazil). For each day, the daily clearness index from Meteonorm (2012) was used to evaluate the incident solar radiation. The mean daily efficiency was obtained for each day and, subsequently, for each month of the year. In addition to the instantaneous and mean efficiency, the instantaneous and mean values of incident solar radiation, absorbed solar radiation and useful gain were also determined.

Figure 1 illustrates the global, beam and diffuse components of the solar radiation along the year. As expected, for points where the global radiation increases the diffuse radiation decreases. For the global solar radiation, the maximum value was observed for February (21.37 MJ/m<sup>2</sup>) and October (21.15 MJ/m<sup>2</sup>), the minimum value was for the month of June (14.99 MJ/m<sup>2</sup>). For the diffuse, the maximum value was for the months of January (12.04 MJ/m<sup>2</sup>) and December (11.51 MJ/m<sup>2</sup>), the minimum value was for the months of June (5.68 MJ/m<sup>2</sup>) and July (5.87 MJ/m<sup>2</sup>).

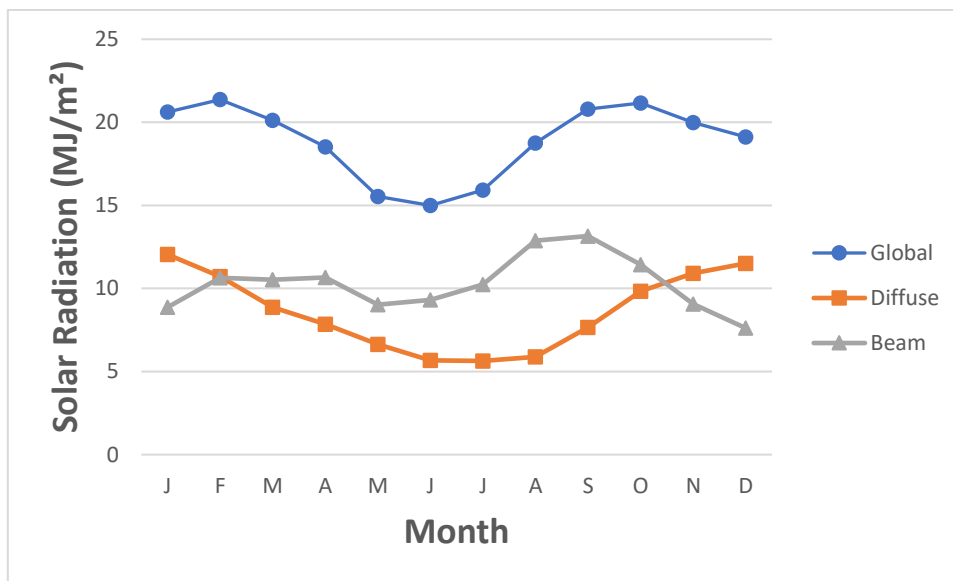


Figure 1. Annual solar radiation.

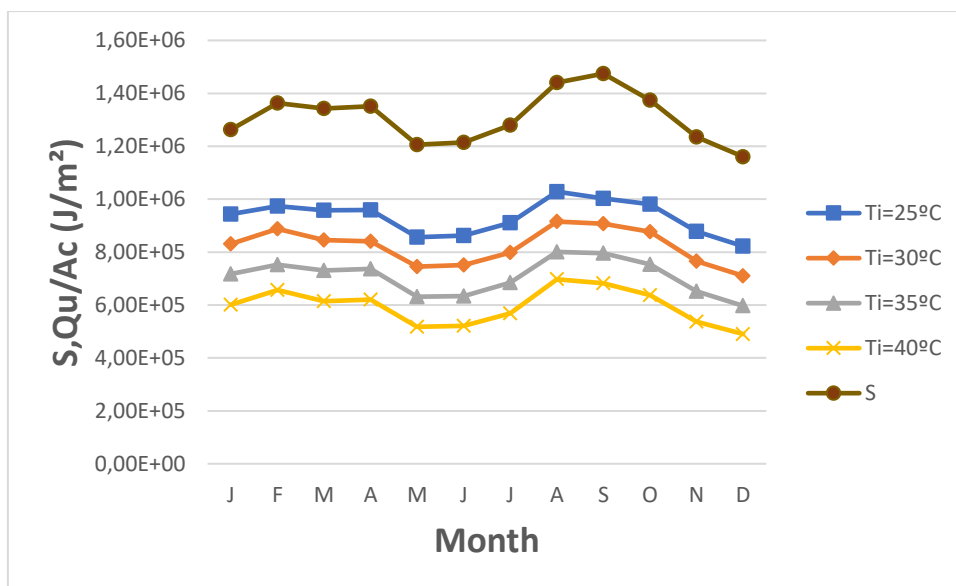


Figure 2. Annual absorber solar radiation and annual useful of the collector for several inlet temperatures.

In Figure 2 it is possible to observe a comparison between the absorbed solar radiation and the useful gain, both for the all months of the year. The useful gain was observed for different inlet temperatures from 25°C to 40°C. For the

absorber solar radiation, just one curve was made since this variable does not depend on the inlet temperature, its only depend on the geometric conditions. It can be observed that all the curves, both absorber solar radiation and useful gain, have the same behavior with minimum values during the winter, which occurs from June to September. The useful gain increases with the decrease of the inlet temperature, this behavior is due to: for a given absorbed solar radiation by the plate, it is possible for the fluid to reach a higher temperature at the outlet, increasing the amount of energy absorbed by the fluid and increasing the useful gain.

Figure 3 shows the behavior of the efficiency throughout the year for the different inlet temperatures. As expected, the same behavior of the useful gain was observed on the efficiency, with the increase of the inlet temperature the efficiency had a decrease. That is justified due to the efficiency be the reason between the useful gain and the incident radiation, without modifying the incident radiation the efficiency and useful gain tends to have a similar behavior.

In addition, in Figure 3, it was noted that the lower values of the efficiency were found during the winter. Observing the behavior throughout the year, for 25°C, the efficiency remained with nearly values, although with the increase of the inlet temperature the efficiency starts to decline on the months from May to July. Comparing the efficiency between the inlet temperatures the results showed a mean increase of 18% between 25°C and 30°C, 23% between 30°C and 35°C, 34% between 35°C and 40°C.

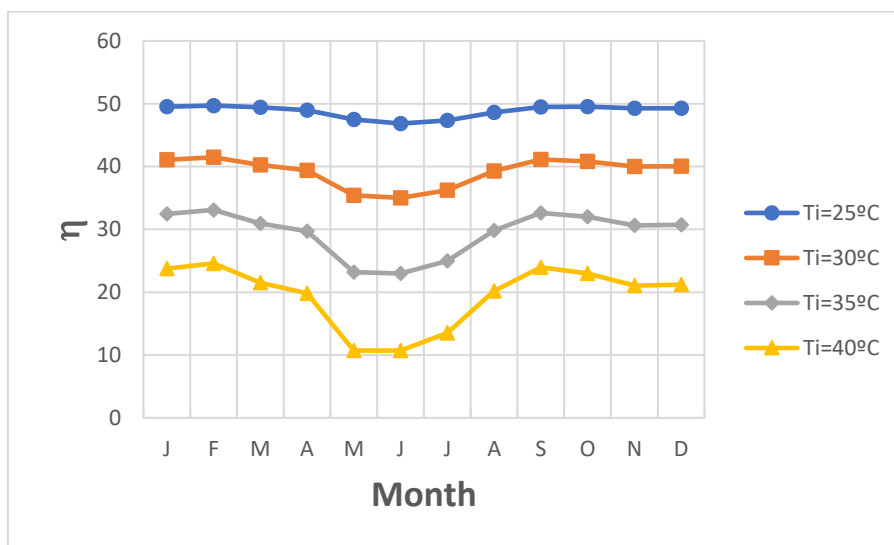


Figure 3. Collector efficiency for several inlet temperatures.

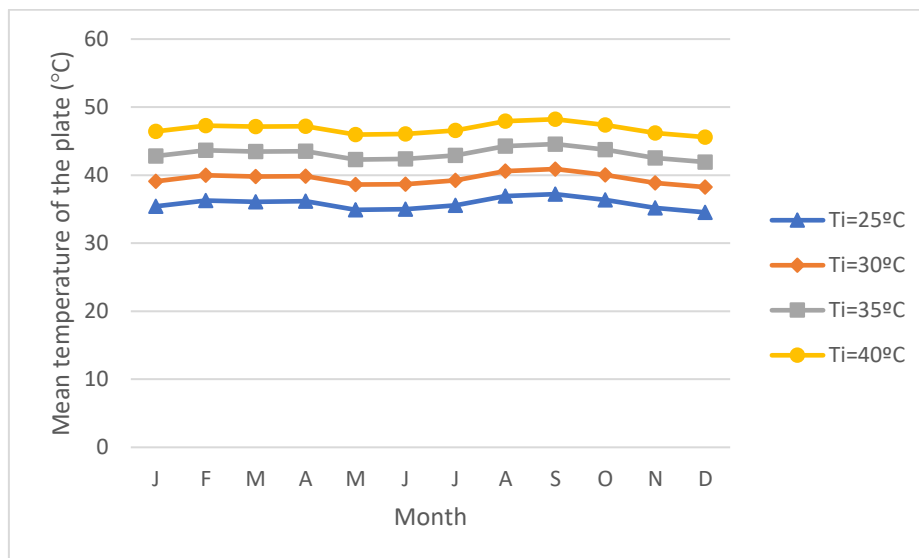


Figure 4. Mean temperature of the plate for several inlet temperatures.

Figure 4 presents the variation of the mean temperature of the plate for distinct inlet temperatures. With the increase of the inlet temperature, the mean temperature of the plate has also showed an increase on its values, this occurs for the reason that when the fluid enters with higher temperature, the heat losses from the plate to the fluid decreases, enabling

the plate to reach higher temperatures. It is possible to see that for all the curves, the mean temperature presented a small variation on the values during the year. In addition, for all inlet temperatures, the mean temperature showed lower values from May to July.

Figure 5 shows the fitted thermal efficiency curve as a function of the reduced temperature parameter  $\Delta T/I$  parameter, built with all the evaluated inlet temperatures (25, 30, 35 and 40°C). The highest thermal efficiency is achieved when  $T_i = T_a$  (which ideally means no loss to surroundings), i.e., zero value of the abscissa Choudhary *et al* (2021). The maximum efficiency obtained is 52.9%. The abscissa 0.02 corresponds to the average value for a bath, with an efficiency of 46.2%.

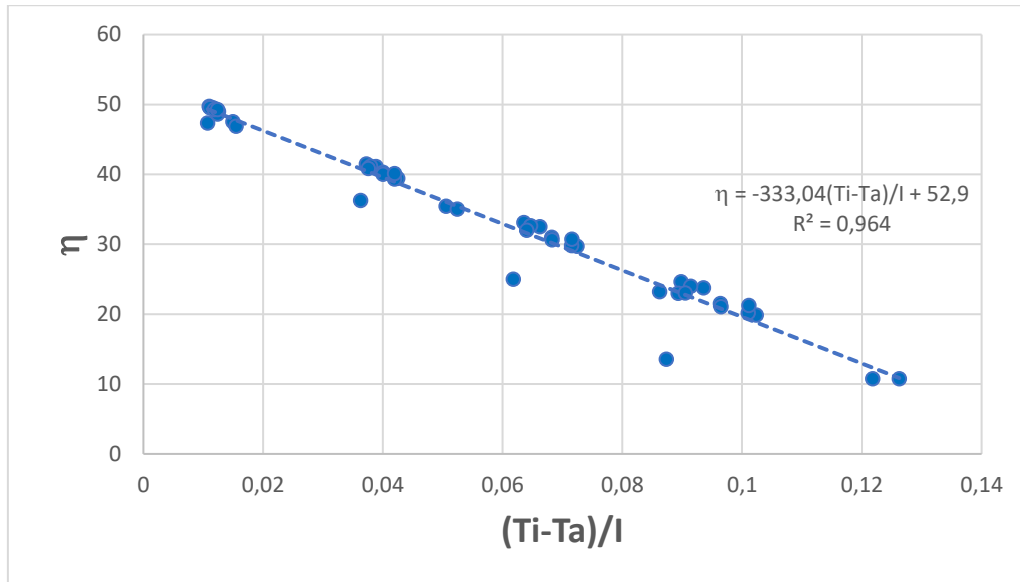


Figure 5. Regressed efficiency equation for several inlet temperatures.

It is worth mentioning the good agreement obtained between the data and the fit adjustment for the different inlet temperatures, with  $R^2 = 0.964$ .

#### 4. CONCLUSIONS

This paper presented a study of a flat plate solar collector in order to investigate the influence of the inlet temperature on the efficiency and the mean temperature of the collector. It was used variation of parameters along the sunlight hours of the day and along for all days of the year. With these variations, it was possible to develop a mean of the day and, posteriorly, a mean for each month, which would represent this study during the year.

It was demonstrated that the inlet temperature plays an importance role on the efficiency and the mean temperature. The mean plate temperature increases with the inlet temperature, and the useful gain and the efficiency decrease with the inlet temperature. The mean temperature has a significant influence on the heat losses; the higher the temperature, the higher the heat losses, due to the higher difference related to ambient temperature. The useful gain is reduced, resulting in lower efficiency.

It was also showed that the absorbed solar radiation has a direct influence on the efficiency since both had similar behavior, a decreasing during winter, and the same can be said for the global solar radiation. The seasonal change during the year occurs due to the changing of the inclination of the earth with respect to the sun, this modification, especially on winter, tends to decrease the incident solar radiation on the local, therefore also decreasing the absorbed radiation.

It was found a maximum efficiency of 52.9% for the solar collector with the configuration proposed. The efficiency evaluated at the average value of bath was 46.2%. The efficiency could be increased by modifying the geometry of the solar collector or using nanofluids.

#### 5. ACKNOWLEDGEMENTS

This study was financing in part by the Coordenação de Aperfeiçoamento de Pessoal de Nível Superior - Brasil (CAPES) - Finance Code 001. The authors are also thankful to the PUC Minas, FAPEMIG, and CNPq.

## 6. REFERENCES

- Beckman, W., Klein, S., and Duffie, J. (1977). *Solar Heating Design by the f-Chart Method*. Wiley Interscience, New York. Brandemueh.
- Bhowmik, H., Amin, R., 2017. Efficiency improvement of flat plate solar collector using reflector. *Energy Reports*, v.3, p. 119-123.
- Choudhary, S., Sachdeva, A., Pramod K. 2021. Time-based analysis of stability and thermal efficiency of flat plate solar collector using iron oxide nanofluid. *Applied Thermal Engineering*, v. 183, 115931.
- Copper, P. (1969). The absorption of radiation in solar stills. *Solar Energy*, 12:333–346.
- Diego-Ayala, U., Carrillo, J.G., 2016. Evaluation of temperature and efficiency in relation to mass flow on a solar flat-plate collector in Mexico. *Renewable Energy*, v. 96, p.756-754.
- Duffie, J. and Beckman, W. (2013). *Solar Engineering and Thermal Processes*. John Wiley & Sons, New Jersey, 4th edition.
- Erbs, D., Klein, S., and Duffie, J. (1982). Estimation of the diffuse radiation fraction for hourly, daily and monthly-average global radiation. *Solar Energy*, 28:293–302.
- He, Q., Zeng, S., Wang, S., 2015. Experimental investigation on the efficiency of flat-plate solar collectors with nanofluids. *Applied Thermal Engineering*, v. 88, p. 165-171.
- Garcia, R.P., Oliveira, S.D.R., Scalon, V.L., 2019. Thermal efficiency experimental evaluation of solar flat plate collectors when introducing convective barriers. *Solar Energy*, v. 182, p. 278-285.
- Maia, C.B., Ferreira, A.G., Hanriot, S.M., 2014. Evaluation of a tracking flat-plate solar collector in Brazil. *Applied Thermal Engineering*, v. 73, p. 954-962.
- Meteonorm, Software of Global Meteorological Database for Engineers, Planners and Education, 2012.
- Müller, S., Giovannetti, F., Reineke-Koch, R., Kastner, O. Hafner, B., 2019. Simulation study on the efficiency of thermochromic absorber coatings for solar thermal flat-plate collectors. *Solar Energy*, v. 188, p. 865–874.
- Sözen, A., Menlik, T., Ünvar, S., 2008. Determination of efficiency of flat-plate solar collectors using neural network approach. *Expert Systems with Applications*, v. 35, p. 1533–1539
- Tong, Y., Chi, X., Kang, W., Cho, H., 2020. Comparative investigation of efficiency sensitivity in a flat plate solar collector according to nanofluids. *Applied Thermal Engineering*, v. 174, 115346.
- Tyagi, H., P. Phelan, R. Prasher, R. 2009. Predicted efficiency of a low-temperature nanofluid-based direct absorption solar collector, *Journal of Solar Energy Engineering*, 131 (4), 041004.

## 7. RESPONSIBILITY NOTICE

The authors are the only responsible for the printed material included in this paper.